BCMA targets bispecific fusion protein for induction of NK cell activity against multiple myeloma

Wei Xu
China Pharmaceutical University
Yang Wang
China Pharmaceutical University
Hui Li
China Pharmaceutical University
Min Wang
China Pharmaceutical University
Juan Zhang (juancpu@126.com)
China Pharmaceutical University https://orcid.org/0000-0002-1475-719X

Research Article

Keywords: BFP, BCMA, MICA, NKG2D, immune surveillance, immunotherapy

Posted Date: March 23rd, 2021

DOI: https://doi.org/10.21203/rs.3.rs-351031/v1

Abstract

Purpose

Multiple myeloma (MM) is the second most common hematological malignancy, and B-cell maturation antigen (BCMA) is a highly regarded target of MM research. In tumors, the natural killer (NK) cell receptor NK group 2, member D (NKG2D), and its ligand MHC class I-related chain A (MICA) play important roles in immune surveillance and killing. We developed a bispecific fusion protein (BFP) that targeted NKG2D and BCMA, which may be useful for the MM therapeutic market.

Methods

The Homo MICA extracellular domains (hMICA) α1-3 or α1-2 were fused to the end of the single chain antibody (ScFv) 2A9 with the flexible linker (G4S), which formed 2A9-MICA and 2A9-MICAα1-2. These were further identified using sodium dodecyl sulfate polyacrylamide gel electrophoresis (SDS-PAGE) and western blotting (WB). The dual-targeting specificity was characterized using Surface Plasmon Resonance (SPR) technology and a flow cytometry assay. In addition, a cytotoxicity assay showed that the design of BFP mediated the lysis of MM cells. Further, in MM-bearing nude mice, the anti-tumor effect and the ability to activate NK cells within tumor tissues of BFP were verified.

Results

Compared with 2A9-MICA, 2A9-MICAα1-2 had a stronger affinity to BCMA and NKG2D, which mediated cytotoxicity of NK effector cells against MM cells. *In vivo*, 2A9-MICAα1-2 showed superior anti-MM efficacy, significantly reduced malignancy, effectively activated $CD56^{+}TNF\text{-}\alpha^{+}$ NK cells, and promoted immune infiltration within the tumor environment.

Conclusion

After we evaluated aspects of 2A9-MICA and 2A9-MICAα1-2 comprehensively, we concluded that 2A9-MICAα1-2 deserves further study and investigation, and it provides a possible strategy for immunotherapy that targets MM.

Highlights

- MM cells highly express BCMA;
- 2A9-NKG2DLs are bispecific fusion proteins that target BCMA and NKG2D;
- After 2A9-NKG2DLs binds to MM cells, NK cells are zoomed to the area of the tumor and activated to exert cytotoxicity against $BCMA^{+}$ malignant cells through the NKG2DLs/NKG2D pathway, and this releases cytokines, IFN-γ, and TNF-α, or the spontaneous cytotoxic molecules perforin and granzyme.

Introduction

Multiple myeloma (MM) is the second most common hematological malignancy in the U.S. and Europe. It is also a terminally differentiated plasmacytoma that is characterized by the uncontrolled proliferation of monoclonal plasma cells in the bone marrow that interferes with the normal production of blood cells. This leads to overproduction of immunoglobulin and immunosuppression, which ultimately leads to osteolysis and end-organ (such as kidney) damage. In the U.S., the lifetime risk of getting multiple myeloma is 1 in 132 (0.76%), and the American Cancer Society's estimates for MM for 2021 are that about 34920 new cases will be diagnosed and about 12410 deaths are expected to occur (Kumar et al. 2017).

At present, the main approaches to MM treatment include chemotherapy, protease inhibitors (such as Bortezomib), immunomodulatory agents (such as Lenalidomide), corticosteroids, stem cell transplantation (SCT), and monoclonal antibodies, such as Elotuzumab, which targets signaling lymphocytic activation molecule F7 (SLAMF7), and Daratumumab, which targets CD38) (Touzeau et al. 2017). Among these treatments, SCT plus chemotherapy has various side effects, and relapse is common; clinically, combined use of protease inhibitors and immunomodulatory agents must be arranged based on the patients' condition, and therapeutic monoclonal antibodies (mAbs) are unaffordable for most people. In addition, some targets of mAbs are not specific enough; they may express on normal tissue cells. For these reasons, the development of MM immunotherapy has been frustrated.

B cell maturation antigen (also named as BCMA, CD269, TNFRSF 17), which belongs to the tumor necrosis factor receptor superfamily, is a potential target for its specificity. BCMA is a plasma cell-specific antigen, which is mainly expressed in MM cell lines, malignant plasma cells, and plasmacytoid dendritic cells, but not in naive and most memory B cells, germinal centers, and normal tissue cells (Hipp et al. 2017). A proliferation-inducing ligand (APRIL), which is the high affinity ligand of BCMA, promotes human MM growth and immunosuppression in the bone marrow microenvironment through many pathways after it is combined with BCMA (Tai et al. 2016). At the moment, there are three mainstream strategies: chimeric antigen receptor T-cell (CAR-T) immunotherapy, antibody-drug conjugates (ADC), and bispecific antibodies (BsAb). Some have achieved impressive clinical results, such as bb2121, LCAR-B38M, AMG420, and GSK2857916 (BiTE Therapy Active in Multiple Myeloma 2019; Cho et al. 2018; Cohen et al. 2019; Raje et al. 2019; Shah et al. 2020; Tai et al. 2014; Topp et al. 2020; Trudel et al. 2018; Trudel et al. 2019; Xu et al. 2019; Zhao et al. 2018). Among these, ADCs may lead to cytotoxic side effects, CAR-T can result in cytokine release syndrome (CRS) or neurotoxicity, and BsAb may be wilder to mediate immune cells that kill malignant plasma cells.

Cancer immunoediting includes three component phases: elimination, equilibrium, and escape. Once tumor cells change themselves, for example, from antigen loss or MHC loss, they will escape from immune surveillance and killing to proliferate and to grow (Mittal et al. 2014; Schreiber et al. 2011; Yoshihama et al. 2016). NKG2D is an immune surveillance receptor, which is expressed mostly in human NK cells. After NKG2D binds to its ligands NKG2DLs in the MIC family that consists of MICA and MICB, or in the ULBP family with six members (ULBP1-6), NK cells are activated. NKG2DLs are inducibly expressed

after cellular stress, viral infection, or malignant transformation, which marks “stressed” or “harmful” cells for clearance through $NKG2D^+$ lymphocytes (Guillerey et al. 2016; Lanier 2015; Lazarova and Steinle 2019). However, NKG2DLs are often attacked by proteases and are shed or become soluble, so the tumor cells are not recognized and killed, such as in leukemia, lymphoma, and MM (Dhar and Wu 2018; Paczulla et al. 2019). MM patients displayed intermediate MICA levels that were lower than patients with monoclonal gammopathy of undetermined significance (MGUS), but they exhibited a high expression of endoplasmic reticulum protein 5 (ERp5), which is a protein disulfide isomerase that resulted in MICA shedding and poor prognosis (Jinushi et al. 2008).

In a previous study, we screened the single chain antibody 2A9 that targeted human BCMA by phage display (Wang et al. 2020). Our lab also generated the bispecific antibody cG7-MICA, which targeted a cluster of differentiation 24 (CD24) and NKG2D simultaneously and which exerted excellent efficacy in recruiting and activating NK against hepatocellular carcinoma (Han et al. 2019). Based on the key role of the NKG2DLs/NKG2D pathway in immune surveillance and killing, the highly specific expression of BCMA, and considering the tumor progression caused by shed MICA (sMICA), we fused 2A9 with the extracellular domains α1–3 or α1–2 of MICA (i.e., because the α3 domain is the recognition site of proteases (Ferrari de Andrade et al. 2018)). This resulted in the design of 2A9-MICA and 2A9-MICAα1–2 fusion proteins that stimulated NK cells against MM.

In this study, within 2A9-MICA and 2A9-MICAα1–2, we evaluated the dual-targeting affinity, cytotoxicity, anti-MM efficacy, and the ability to activate NK cells. Our results showed that 2A9-MICAα1–2 had better dual-targeting ability than 2A9-MICA, significantly inhibited tumor growth, and reduced the malignancy of MM. Furthermore, 2A9-MICAα1–2 activated NK cells within tumor tissues effectively in a MM xenograft model. Thus, we hypothesized that the truncated MICA molecule, MICAα1–2, would be more effective in immunotherapy strategy when associated with NK effector cells.

Materials And Methods

Cell culture and materials

Human multiple myeloma cell lines NCI-H929, RPMI-8226, and human Burkitt’s lymphoma cell line Raji that were preserved in our laboratory were cultured in RPMI-1640 medium (Gibco, USA) that contained 10% (v/v) fetal bovine serum (FBS, Gibco, USA). Human natural killer cell line NK-92MI from our lab was cultured in Alpha Minimum Essential Medium (MEM-α, Gibco, USA) with 2 mM L-glutamine, 1.5 g/L sodium bicarbonate, 0.2 mM inositol, 0.1 mM 2-mercaptoethanol, 0.02 mM folic acid, 12.5% (v/v) horse serum (Hyclone), and 12.5% (v/v) FBS. Human embryonic kidney 293 (HEK 293) cells from our lab were cultured in Dulbecco's Modified Eagle Medium (DMEM, Gibco, USA) with 10% (v/v) FBS. All cells were incubated in a humid atmosphere of 5% CO_2 at 37℃. The 4-w-old Balb/c nude mice used in this study were purchased from Comparative Medicine Centre of Yangzhou University (Yangzhou, China). All animals were fed in a specific pathogen-free environment and were treated according to the criteria of the Comparative Medicine Centre of Yangzhou University.

Construction, expression, purification, and identification of 2A9-MICA and 2A9-MICAα1-2

The single chain antibody 2A9 that targeted human BCMA was screened from the CPU2 phage display library of murine single-chain antibodies using phage display technology (Wang et al. 2020). The cDNA sequences of 2A9 and human MICA extracellular domains (residues 24–307, Uniprot identifier: Q29983) were optimized to HEK 293-preferred codons at GenScript (Nanjing, China). Then, we spliced 2A9 with hMICA and 2A9 with hMICAα1-2 by overlap PCR after digestion with EcoR Ⅰ and Not Ⅰ (Takara, Japan). The recombinant DNA of 2A9, 2A9-MICA, and 2A9-MICAα1-2 were ligated separately to a digested pcDNA 3.0 vector, which formed pcDNA 3.0-2A9, pcDNA 3.0-2A9-MICA, and pcDNA 3.0-2A9-MICAα1-2. Further, these three recombinant eukaryotic expression vectors were transfected into HEK 293 cells with polyethylenimine (PEI). During the culture of transfected host cells, the culture supernatants were collected to purify proteins 2A9, 2A9-MICA, and 2A9-MICAα1-2 by affinity chromatography on a His Trap high-performance column (GE Healthcare, Sweden), which was followed by analysis using SDS-PAGE (15% gel for 2A9; 10% gel for 2A9-MICA and 2A9-MICAα1-2) and Western blot assay (anti-His antibody for 2A9, 2A9-MICA, and 2A9-MICAα1-2, Proteintech Group, Wuhan, China; anti-MICA antibody for 2A9-MICA and 2A9-MICAα1-2, SunBio Technology, Nanjing, China).

Quantitative real-time polymerase chain reaction (qRT-PCR)

RNAs were isolated using TRIeasy™ Total RNA Extraction Reagent (Yeasen, Shanghai, China) and transcribed into cDNA using Hifair® Ⅱ 1st Standard cDNA Synthesis Kit (Yeasen, Shanghai, China). Gene transcripts were detected using an Applied Biosystems 7300 Plus Real-Time PCR System (Thermo Fisher Scientific, USA) and Hieff UNICON® qPCR SYBR Green Master Mix (High Rox, Yeasen, Shanghai, China) and gene-specific primers (BCMA up: 5'ACCTTGTCAACTTCGATGTTCTT3', BCMA down: 5'CAGAGAATCGCATTCGTTCCTT3'; GAPDH up: 5'TGTGGGCATCAATGGATTTGG3', GAPDH down: 5'ACACCATGTATTCCGGGTCAAT3'). The GAPDH internal control was used for normalization. Average fold-change values of gene expression were calculated from triplicate measurements using the $\Delta\Delta$CT method.

Immunoblot

Immunoblots were performed according to standard procedures using anti-human-BCMA (SunBio Technology, Nanjing, China) and anti-GAPDH (Proteintech Group, Wuhan, Chima) antibodies and HRP-conjugated secondary reagents (goat-anti-rabbit IgG and goat-anti-mouse IgG, all from Proteintech Group).

Analysis of binding affinity using flow cytometry and surface plasmon resonance

To evaluate the binding affinity of the fusion proteins to $BCMA^+$ multiple myeloma cells, NCI-H929 and RPMI-8226 were used as experimental objectives and Raji was the negative control; 1×10^6 cells of each were pre-incubated with PBS that contained 2% (v/v) FBS and 1000 nM protein samples or an isotype control antibody at 4°C for 1 h. Cells were then incubated with mouse His-tag monoclonal antibody and

CoraLite488-conjugated Affinipure goat anti-mouse IgG (H+L) (Proteintech Group, Wuhan, China) for 1 h at 4℃. The cells were analyzed by flow cytometry (MACSQuant, Miltenyi Biotec, Germany).

The binding kinetics of fusion proteins 2A9-MICA and 2A9-MICAα1-2 to the NKG2D protein were measured with a Biacore system (Biacore X100, GE Healthcare, Sweden). Human NKG2D protein (Novoprotein, Shanghai, China) was coupled covalently to the CM5 sensor chip (GE Healthcare, Sweden), and soluble 2A9-MICA or 2A9-MICAα1-2 was injected at gradient concentrations into the running buffer (HBS-EP, pH 7.4). One flow cell of the sensor chip was used as a control, another flow cell was the experimental channel, and Gly-HCl (pH 2.0) was used to elute the analyte. The affinity of fusion proteins with NKG2D was evaluated with Biacore X100 Evaluation software: the equilibrium dissociation constant (KD) = dissociation rate constant (kd) / association rate constant (ka).

NKG2D expression on NK-92MI and cytotoxicity assay

NK-92MI cells were stained with PE-anti-human CD314 (NKG2D) antibody (Biolegend, USA) and analyzed by flow cytometry to determine NKG2D expression. A Lactate Dehydrogenase (LDH) Cytotoxicity Assay Kit (Beyotime, Shanghai, China) was used to detect LDH release from target cells in a cytotoxicity assay. The target cells NCI-H929, RPMI-8226, and Raji were co-cultured with various amounts of NK-92MI cells for 6 h at 37℃ in the presence of different treatments; 60 μL of the co-culture supernatants from each well was then analyzed for LDH activity. In addition to the experimental groups, a spontaneous LDH release in effector or target cells and a maximum LDH release in target cells were also prepared. Absorbance values were used to calculate the rate of cell lysis. Cell lysis (%) = [(experimental-effector cells spontaneous-target cells spontaneous)/(target cells maximum-target cells spontaneous)]×100%.

Stability of fusion proteins

2A9, 29-MICA, and 2A9-MICAα1-2 (2 mg/mL) were stored at 4℃ and -20℃ for 5 d, and then SDS-PAGE was performed to detect the degradation of proteins under different short-storage conditions to evaluate their physical stability. 2A9, 2A9-MICA, and 2A9-MICAα1-2 were diluted with filtered human plasma to 1000 nM and kept at 37°C for 1, 3, 5, or 7 d. Flow cytometry was used to detect the binding of proteins in human plasma at 37℃ to NCI-H929 cells for a preliminary analysis of their biological stability.

NCI-H929 xenograft model

The NCI-H929 cells ($1x10^7$) were injected subcutaneously into the right dorsal flank of each 4-w-old Balb/c nude mouse (Hipp et al. 2017; Seckinger et al. 2017). When the average tumor volume reached 100 mm^3, all the tumor-bearing mice were divided randomly into four groups of five mice each; fusion proteins or other treatments were administered to each group according to established protocols. The anti-myeloma efficacy of fusion proteins 2A9-MICA and 2A9-MICAα1-2 (i.v., 2 mg/kg, q.2d.) was estimated compared with Rd treatment (i.g.; R: Lenalidomide, 3 mg/kg, q.d.; d: Dexamethasone, 5 mg/kg, d1-4/d9-12), and the saline-treated mice were set as the vehicle control. During the administration, $5×10^6$ NK-92MI cells were injected intravenously into every experimental mouse (q.6d.) (Swift et al. 2012; Zhu et

al. 2017). Tumor growth and body weight of mice were monitored by caliper measurements every other day (i.e., Tumor volume: $V=LW^2/2$, L: the longest diameter of tumor, W: maximum transverse diameter of vertical direction). The study was terminated on day 22 after administration when tumors of vehicle-treated mice exceeded 2000 mm^3. Tumor tissues and organs (i.e., heart, liver, spleen, lung, and kidney) of mice were prepared for further analysis.

Immunohistochemistry, immunofluorescence, and hematoxylin-eosin (H&E) staining

Tumor tissues from experimental mice and spleens of normal and experimental mice were fixed by 4% paraformaldehyde and embedded in paraffin, and paraffin blocks were cut into 2 μm sections. For immunohistochemical (IHC) staining, tumor sections were incubated with anti-Ki-67 antibody (Cell Signaling Technology, Boston, USA) and anti-BCMA antibody (Proteintech Group, Wuhan, China) separately, followed by HRP-conjugated goat anti-rabbit secondary antibody, then detected with DAB Immunohistochemistry Color Development Kit (Sangon Biotech, Shanghai, China). For immunofluorescence (IF) staining, tumor sections were incubated with anti-human CD56, anti-TNF-α antibodies (Novus Biological, USA), and Alexa Fluor® 647 AffiniPure Goat Anti-Rabbit IgG (H+L) (FMS-Rbaf64701, FcMACS, NanJing, China). Spleen sections were used for H&E staining to evaluate the splenic damage and toxicity of fusion proteins. Along with these assays, images of IHC and H&E staining sections were captured with an upright biological microscope (BX53, Olympus, Japan) or inverted fluorescence microscope (ECLIPSE Ts2R, Nikon, Japan). Fluorescent images were observed with a confocal laser scanning microscope (CLSM, LSM800, Zeiss, Germany) and processed using ZEN imaging software.

Statistical Analysis

Data were analyzed using SPSS 22.0 and GraphPad Prism 6. Differences between multiple groups were estimated by a Student t test, and a P-value < 0.05 was considered to be statistically significant.

Results

Construction and identification of 2A9, 2A9-MICA, and 2A9-MICAα1-2

The DNA sequences of 2A9, 2A9-MICA, and 2A9-MICAα1-2 were recombined into pcDNA 3.0, then these special recombinant plasmids were transfected into HEK 293 cells for expression (Fig. 1a, b). SDS-PAGE and WB showed that the proteins of interest were homogenous with the expected molecular weight of 28 kDa for 2A9, 66 kDa for 2A9-MICA, and 53 kDa for 2A9-MICAα1-2 (Fig. 1c, d, e).

Dual-targeting ability of 2A9-MICA and 2A9-MICAα1-2

The Cancer Cell Line Encyclopedia (CCLE) database described the RNA expression of TNFRSF 17, and qPCR results showed that NCI-H929 expressed TNFRSF 17 at a much higher level than RPMI-8226, which was also indicated in an immunoblot at the protein level (Fig. 2a, b, c). In summary, NCI-H929 was a

BCMA highly expressed cell line, but RPMI-8226 expressed a lower level of BCMA. The binding of 2A9, 2A9-MICA, and 2A9-MICAα1-2 to $BCMA^+$ MM cell lines NCI-H929, RPMI-8226, and $BCMA^-$ cell line Raji was evaluated with flow cytometry. There was no expression of NKG2D on the above-mentioned tumor cell lines (Fig. 2d), and binding of NKG2D ligands MICAα1-3 and MICAα1-2 to tumor cell lines was also not detected (Fig. 2e). 2A9-MICA and 2A9 had a similar binding capacity to RPMI-8226 and NCI-H929, but no binding to Raji, whereas 2A9-MICAα1-2 exhibited a higher binding ability that was almost 60% to RPMI-8226 and 90% to NCI-H929 (Fig. 2f). The affinity of 2A9-MICA and 2A9-MICAα1-2 with human NKG2D was measured by SPR. 2A9-MICAα1-2 exhibited a higher affinity to NKG2D [ka (1/Ms): 1.58E+05, kd (1/s): 0.005733, KD (M): 3.63E-08], which was stronger than that of 2A9-MICA [ka (1/Ms): 5.10E+04, kd (1/s): 0.004578, KD (M): 8.99E-08] (Fig. 2g). In short, fusion proteins 2A9-MICA and 2A9-MICAα1-2 were both able to target NKG2D and BCMA at the molecular and cellular levels, respectively. Furthermore, 2A9-MICAα1-2 exhibited a stronger dual-targeting ability.

2A9-MICAα1-2 effectively mediated NK-92MI cytotoxicity to $BCMA^+$ MM cells

The cell surface expression of NKG2D on NK-92MI cells was identified through a commercial antibody that was specific for human NKG2D, and there was nearly a 60% NKG2D-positive area (Fig, 3a). To investigate NKG2D-mediated cytotoxicity, NCI-H929, RPMI-8226, and Raji cells were used as target cells, and the identified NK-92MI cells were used as effector cells. We first set different E:T (Effector:Target) ratios to examine tumor cell-lysis in the presence of NK-92MI cells and an optional concentration of 2A9, 2A9-MICA, and 2A9-MICAα1-2. We found that fusion proteins, especially 2A9-MICAα1-2, triggered higher cytotoxicity to RPMI-8226 and NCI-H929 cells in an E:T-dependent manner (Fig. 3b, c, d). Then, we maintained a definite E:T of 10:1 and determined cell lysis using gradient concentrations of treatments, and we found that 2A9-MICAα1-2 exhibited a concentration-dependent cytotoxicity to the above two $BCMA^+$ MM cells (Fig. 3e, f, g). Earlier studies showed that the cell lysis of 2A9-MICA against BCMA-knockdown-NCI-H929 cells was reduced significantly compared with NCI-H929, and the cytotoxicity of some antibody-MICA fusion proteins against corresponding target cells was also inhibited obviously when hMICA was added (Han et al. 2019; Wang et al. 2016b; Wang et al. 2020). In short, we concluded that fusion proteins, 2A9-MICA and 2A9-MICAα1-2, mediated cytotoxicity through BCMA/2A9 and MICA/NKG2D pathways.

2A9-MICAα1-2 exhibited superior anti-myeloma efficacy in NCI-H929-bearing mice model

To evaluate the anti-MM efficacy of fusion proteins, NCI-H929 cells were inoculated to the armpit of Balb/c mice subcutaneously. The tumor-bearing mice were divided randomly into four groups and treated with different drugs (i.e., Saline, 2A9-MICA, 2A9-MICAα1-2, and Rd treatment) (Fig. 4a). According to the biological and physical stability of fusion proteins, we administered every 2 d (Supplementary Fig. 1). During administration, tumor volume was monitored (Fig. 4c); the growth of 2A9-MICAα1-2 and Rd treatment groups was obviously slower than others and, at the end point of the experiment, we preserved all tumors from each group (Fig. 4b). Tumor weight (Fig. 4d) was used to describe tumor inhibition (Fig. 4e), and we found that 2A9-MICAα1-2 reduced tumor burdens significantly by 51.7%, which was higher

than the reduction of 28.3% for 2A9-MICA and 41.1% for Rd treatment. In addition, we monitored the body weight of NCI-H929-bearing mice and the weight of main organs. There were no differences between experimental groups, which meant that there was no systematic toxicity from fusion proteins (Fig. 4f, g and Supplementary Fig. 2).

2A9-MICAα1-2 effectively reduced malignancy of MM and fully activated NK cells

To demonstrate the anti-MM effect of fusion proteins, especially 2A9-MICAα1-2, immunohistochemistry of human Ki-67 and BCMA was performed to identify the malignancy in NCI-H929 tumor tissues (Fig. 5a, c). 2A9-MICAα1-2 reduced the malignancy of MM effectively compared with Rd positive drugs (Fig. 5b, d). Furthermore, immunofluorescence was used to monitor the infiltration, activation, and cytokine release of NK cells. After treatment with 2A9-MICAα1-2, the proportion of $CD56^{+}TNF\text{-}\alpha^{+}$ human NK cells was higher than in groups treated with 2A9-MICA and Rd positive drugs (Fig. 5e, f), which meant that 2A9-MICAα1-2 recruited and collected activated NK cells successfully. In summary, compared with 2A9-MICA and Rd treatment, 2A9-MICAα1-2 showed superior anti-myeloma efficacy, excellent ability to activate NK effector cells, and increased immune infiltration *in vivo*.

Discussion

In this study, we designed the two bispecific fusion proteins 2A9-MICA and 2A9-MICAα1-2 by fusing the extracellular domains of hMICA α1-3 or α1-2 with the C-terminus of 2A9 through a flexible linker (Kellner et al. 2012; von Strandmann et al. 2006). 2A9 was screened from the CPU2 phage display library of murine single-chain antibodies using phage display technology. MICA, which is a major histocompatibility complex class I-related chain A, has three domains in its extracellular region. Among these domains, α1 and α2 bound to NKG2D, and α3 was recognized by ERp5 and other proteases. Therefore, cell bound MICA often be shed to sMICA, which results in the progression and development of tumors. 2A9-MICA and 2A9-MICAα1-2 utilized the specific expression of BCMA to display MICA or MICAα1-2 on the surface of multiple myeloma cells; in this way, $NKG2D^{+}$ lymphocytes, especially NK cells, recognized and killed $BCMA^{+}$ tumor cells in MM.

As we know, many immunotherapy programs focus on T cells because of their powerful killing ability against tumor cells. But, the cytotoxicity of T cells derives from the presentation of MHC antigens of target cells. After tumor cells change or lose the expression of MHC antigens, they can escape from being killed (Jinushi et al. 2008; Paczulla et al. 2019; Yoshihama et al. 2016). On the other hand, NK cells, which are a kind of innate immune cells, are activated without antigens and produce a rapid immune response. Therefore, compared with cytotoxic T cells, NK cells were activated easily, especially when tumor antigens were lost or shed.

In our research, we used NK cells as the core force to kill multiple myeloma. We assessed and compared 2A9-MICA and 2A9-MICAα1-2 through a series of systematic studies that was intended to screen fusion

proteins with certain expression advantage, excellent anti-MM effect, and the ability to activate NK cells. We aimed to provide a reference for the MM market where the therapeutic landscape is difficult to resolve.

First, we constructed and expressed 2A9-MICA and 2A9-MICAα1-2. To analyze the binding and affinity of fusion proteins, we performed flow cytometry and surface plasmon resonance. Surprisingly, 2A9-MICAα1-2 showed superior binding ability to $BCMA^+$ MM cell lines and better affinity to the human NKG2D protein; the select dual-targeting ability was the basis of the function of fusion proteins. Next, we chose NK-92MI cells as effector cells to assess whether 2A9-MICA or 2A9-MICAα1-2 mediated cytotoxicity against $BCMA^+$ myeloma cells effectively, and we found that 2A9-MICAα1-2 caused higher target cell-lysis by NK-92MI, especially for NCI-H929 cell line. Previous studies showed that the process by which MICA fusion proteins stimulated activation of NK cells was blocked by excess rMICA (Wang et al. 2016b), so we concluded that the activation of NK-92MI cells and the cell lysis against target cells were derived from the MICA/NKG2D pathway.

Further, we investigated the anti-MM effect of 2A9-MICAα1-2 in a NCI-H929 xenograft mouse model. The combination of Lenalidomide and Dexamethasone therapy, the first-line treatment option, was chosen as positive drugs. The Balb/c nude mice are immunodeficient in the absence of T cells and, during the administration, we injected human NK-92MI cells as a protocol to assess the activation by 2A9-MICAα1-2 *in vivo*. 2A9-MICAα1-2 significantly reduced tumor size (i.e., tumor inhibition was 51.7%) and tumor malignancy, as shown in immunohistochemistry of Ki-67 and BCMA. At the same time, no visible systemic toxicity or spleen damage was detected in this model, which meant that 2A9-MICAα1-2 was safe to administer.

Also, we analyzed the activation of NK cells within tumor tissues. 2A9-MICAα1-2 activated $CD56^+$ human NK cells effectively and promoted the immune infiltration of TNF-α. In addition, 2A9-MICAα1-2 recruited and collected activated NK cells together more effectively, which may have caused a stronger immune response. In other words, 2A9-MICAα1-2 had more potential than 2A9-MICA to activate NK cells.

To solve the shedding of MICA, Lucas et al (Ferrari de Andrade et al. 2018) explored antibodies that targeted α3 of MICA and MICB, which blocked the site of ERp5 action. Our design was to engineer and to retouch BCMA positive MM cells through bispecific fusion proteins and to activate NK cells through the MICA/NKG2D pathway.

In summary, compared with 2A9-MICA, the second generation of the bispecific fusion protein 2A9-MICAα1-2 lacked the α3 extracellular domain of hMICA and completely reduced the risk of shedding by some proteases. Besides, the stronger binding with BCMA positive cells and higher affinity to NKG2D protein allowed 2A9-MICAα1-2 to mediate effector cells that killed target cells. Most importantly, 2A9-MICAα1-2 had superior anti-MM efficacy and reduced the malignancy of tumor tissues significantly; at the same time, it also effectively activated $CD56^+TNF\text{-}\alpha^+$ NK cells and promoted immune infiltration within tumor tissues in a xenograft mouse model. The systemic toxicity and spleen damage were also

considered and monitored in this *in vivo* experiment, which showed that 2A9-MICAα1-2 was relatively safe to administer.

Multiple myeloma is a kind of immune-altered, immunosuppressive tumor, and insufficient immune infiltration is the biggest feature of this type of tumor (Galon and Bruni 2019). A high level of interleukin-10 (IL-10) in serum predicts poor prognosis in multiple myeloma (Wang et al. 2016a). In addition to IL-10, TGF-β and PD-L1 may also contribute to an immunosuppressive microenvironment (Tai et al. 2016). 2A9-MICAα1-2 is designed to promote immune infiltration, but the diversification of cytokines and immunomodulatory factors should be monitored and analyzed in more detail. In future research, we also should pay attention to the structure and conformation of 2A9-MICAα1-2, the clinical application of 2A9-MICAα1-2 in combination with other first line therapies against MM or other BCMA-positive malignant tumors.

Declarations

Acknowledgements We thank Thomas A. Gavin, Professor Emeritus, Cornell University, for help with editing this paper.

Funding This study was supported by grants from the National Natural Science Foundation of China (Grants 81981973223, 81773755) and the National Innovation and Entrepreneurship Training Program for Undergraduate (No.202010316049S).

Compliance with ethical standards

Conflict of interest The authors declare no competing financial interests.

Ethical approval All experimental procedures were conducted in conformity with institutional guidelines for the care and use of laboratory animals in Yangzhou University, Yangzhou, China, and they conformed to the National Institutes of Regulations for the Administration of Affairs Concerning Experimental Animals.

References

BiTE Therapy Active in Multiple Myeloma (2019). Cancer Discov 9:157-158. https://doi.rog/10.1158/2159-8290.Cd-nb2019-001

Cho SF, Anderson KC, Tai YT (2018) Targeting B Cell Maturation Antigen (BCMA) in Multiple Myeloma: Potential Uses of BCMA-Based Immunotherapy. Front Immunol 9:1821. https://doi.rog/10.3389/fimmu.2018.01821

Cohen AD, Raje N, Fowler JA, Mezzi K, Scott EC, Dhodapkar MV (2019) How to Train Your T Cells: Overcoming Immune Dysfunction in Multiple Myeloma. Clin Cancer Res. https://doi.rog/10.1158/1078-0432.Ccr-19-2111

Dhar P, Wu JD (2018) NKG2D and its ligands in cancer. Curr Opin Immunol 51:55-61. https://doi.rog/10.1016/j.coi.2018.02.004

Ferrari de Andrade L et al (2018) Antibody-mediated inhibition of MICA and MICB shedding promotes NK cell-driven tumor immunity. Science 359:1537-1542. https://doi.rog/10.1126/science.aao0505

Galon J, Bruni D (2019) Approaches to treat immune hot, altered and cold tumours with combination immunotherapies. Nat Rev Drug Discov 18:197-218. https://doi.rog/10.1038/s41573-018-0007-y

Guillerey C, Huntington ND, Smyth MJ (2016) Targeting natural killer cells in cancer immunotherapy. Nat Immunol 17:1025-1036. https://doi.rog/10.1038/ni.3518

Han Y et al (2019) CD24 targeting bi-specific antibody that simultaneously stimulates NKG2D enhances the efficacy of cancer immunotherapy. J Cancer Res Clin Oncol 145:1179-1190. https://doi.rog/10.1007/s00432-019-02865-8

Hipp S et al (2017) A novel BCMA/CD3 bispecific T-cell engager for the treatment of multiple myeloma induces selective lysis in vitro and in vivo. Leukemia 31:1743-1751. https://doi.rog/10.1038/leu.2016.388

Jinushi M et al (2008) MHC class I chain-related protein A antibodies and shedding are associated with the progression of multiple myeloma. Proc Natl Acad Sci U S A 105:1285-1290. https://doi.rog/10.1073/pnas.0711293105

Kellner C et al (2012) Fusion proteins between ligands for NKG2D and CD20-directed single-chain variable fragments sensitize lymphoma cells for natural killer cell-mediated lysis and enhance antibody-dependent cellular cytotoxicity. Leukemia 26:830-834. https://doi.rog/10.1038/leu.2011.288

Kumar SK et al (2017) Multiple myeloma. Nature Reviews Disease Primers 3:17046. https://doi.rog/10.1038/nrdp.2017.46

Lanier LL (2015) NKG2D Receptor and Its Ligands in Host Defense. Cancer Immunol Res 3:575-582. https://doi.rog/10.1158/2326-6066.Cir-15-0098

Lazarova M, Steinle A (2019) The NKG2D axis: an emerging target in cancer immunotherapy. Expert Opin Ther Targets 23:281-294. https://doi.rog/10.1080/14728222.2019.1580693

Mittal D, Gubin MM, Schreiber RD, Smyth MJ (2014) New insights into cancer immunoediting and its three component phases–elimination, equilibrium and escape. Curr Opin Immunol 27:16-25. https://doi.rog/10.1016/j.coi.2014.01.004

Paczulla AM et al (2019) Absence of NKG2D ligands defines leukaemia stem cells and mediates their immune evasion. Nature 572:254-259. https://doi.rog/10.1038/s41586-019-1410-1

Raje N et al (2019) Anti-BCMA CAR T-Cell Therapy bb2121 in Relapsed or Refractory Multiple Myeloma. N Engl J Med 380:1726-1737. https://doi.rog/10.1056/NEJMoa1817226

Schreiber RD, Old LJ, Smyth MJ (2011) Cancer immunoediting: integrating immunity's roles in cancer suppression and promotion. Science 331:1565-1570. https://doi.rog/10.1126/science.1203486

Seckinger A et al (2017) Target Expression, Generation, Preclinical Activity, and Pharmacokinetics of the BCMA-T Cell Bispecific Antibody EM801 for Multiple Myeloma Treatment. Cancer Cell 31:396-410. https://doi.rog/10.1016/j.ccell.2017.02.002

Shah N, Chari A, Scott E, Mezzi K, Usmani SZ (2020) B-cell maturation antigen (BCMA) in multiple myeloma: rationale for targeting and current therapeutic approaches. Leukemia. https://doi.rog/10.1038/s41375-020-0734-z

Swift BE et al (2012) Natural killer cell lines preferentially kill clonogenic multiple myeloma cells and decrease myeloma engraftment in a bioluminescent xenograft mouse model. Haematologica 97:1020-1028. https://doi.rog/10.3324/haematol.2011.054254

Tai YT et al (2016) APRIL and BCMA promote human multiple myeloma growth and immunosuppression in the bone marrow microenvironment. Blood 127:3225-3236. https://doi.rog/10.1182/blood-2016-01-691162

Tai YT et al (2014) Novel anti-B-cell maturation antigen antibody-drug conjugate (GSK2857916) selectively induces killing of multiple myeloma. Blood 123:3128-3138. https://doi.rog/10.1182/blood-2013-10-535088

Topp MS et al (2020) Anti-B-Cell Maturation Antigen BiTE Molecule AMG 420 Induces Responses in Multiple Myeloma. J Clin Oncol 38:775-783. https://doi.rog/10.1200/jco.19.02657

Touzeau C, Moreau P, Dumontet C (2017) Monoclonal antibody therapy in multiple myeloma. Leukemia 31:1039-1047. https://doi.rog/10.1038/leu.2017.60

Trudel S et al (2018) Targeting B-cell maturation antigen with GSK2857916 antibody-drug conjugate in relapsed or refractory multiple myeloma (BMA117159): a dose escalation and expansion phase 1 trial. Lancet Oncol 19:1641-1653. https://doi.rog/10.1016/s1470-2045(18)30576-x

Trudel S et al (2019) Antibody-drug conjugate, GSK2857916, in relapsed/refractory multiple myeloma: an update on safety and efficacy from dose expansion phase I study. Blood Cancer J 9:37. https://doi.rog/10.1038/s41408-019-0196-6

von Strandmann EP et al (2006) A novel bispecific protein (ULBP2-BB4) targeting the NKG2D receptor on natural killer (NK) cells and CD138 activates NK cells and has potent antitumor activity against human multiple myeloma in vitro and in vivo. Blood 107:1955-1962. https://doi.rog/10.1182/blood-2005-05-2177

Wang H et al (2016a) High level of interleukin-10 in serum predicts poor prognosis in multiple myeloma. Br J Cancer 114:463-468. https://doi.rog/10.1038/bjc.2016.11

Wang T et al (2016b) A bispecific protein rG7S-MICA recruits natural killer cells and enhances NKG2D-mediated immunosurveillance against hepatocellular carcinoma. Cancer Lett 372:166-178. https://doi.rog/10.1016/j.canlet.2016.01.001

Wang Y et al (2020) BCMA-targeting Bispecific Antibody That Simultaneously Stimulates NKG2D-enhanced Efficacy Against Multiple Myeloma. J Immunother 43:175-188. https://doi.rog/10.1097/cji.0000000000000320

Xu J et al (2019) Exploratory trial of a biepitopic CAR T-targeting B cell maturation antigen in relapsed/refractory multiple myeloma. Proc Natl Acad Sci U S A 116:9543-9551. https://doi.rog/10.1073/pnas.1819745116

Yoshihama S et al (2016) NLRC5/MHC class I transactivator is a target for immune evasion in cancer. Proc Natl Acad Sci U S A 113:5999-6004. https://doi.rog/10.1073/pnas.1602069113

Zhao WH et al (2018) A phase 1, open-label study of LCAR-B38M, a chimeric antigen receptor T cell therapy directed against B cell maturation antigen, in patients with relapsed or refractory multiple myeloma. J Hematol Oncol 11:141. https://doi.rog/10.1186/s13045-018-0681-6

Zhu L et al (2017) Natural Killer Cell (NK-92MI)-Based Therapy for Pulmonary Metastasis of Anaplastic Thyroid Cancer in a Nude Mouse Model. Front Immunol 8:816. https://doi.rog/10.3389/fimmu.2017.00816

Figures

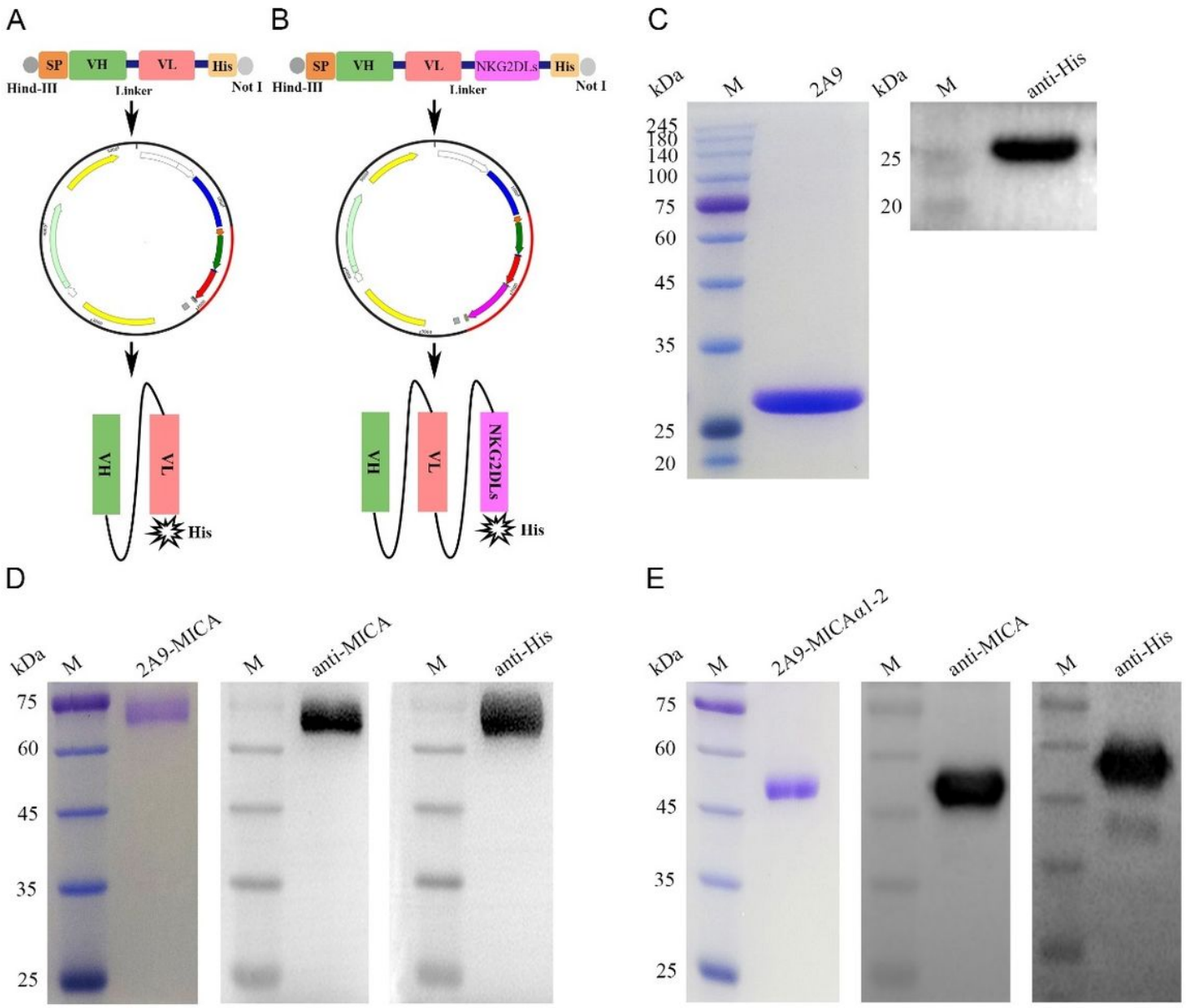

Figure 1

Construction and identification of 2A9, 2A9-MICA, and 2A9-MICAα1-2. a Diagram of the construction and structure of 2A9, 2A9-NKG2DLs. c, d, e SDS–PAGE and non-reducing western blot analysis for the molecular weight and assembly of 2A9 ScFv, 2A9-MICA and 2A9-MICAα1-2. SP means signal peptide, M means protein markers.

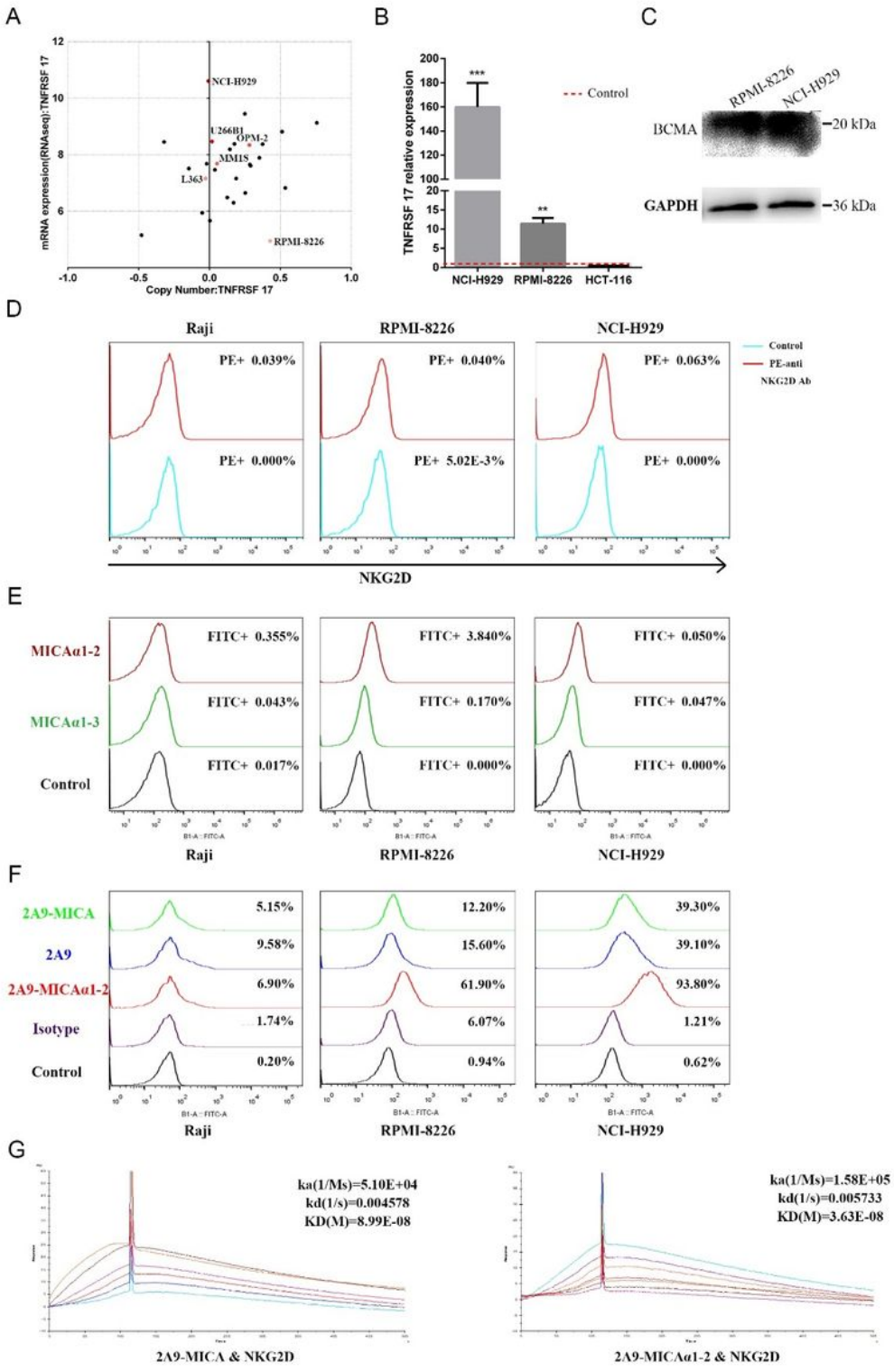

Figure 2

Dual-targeting ability of 2A9-MICA and 2A9-MICAα1-2. a The Cancer Cell Line Encyclopedia (CCLE) database described the mRNA expression of TNFRSF 17 in 27 multiple myeloma cell lines. Among these, the TNFRSF 17 mRNA expression level of NCI-H929 was the highest. b, c The relative expression of TNFRSF 17 in RPMI-8226 and NCI-H929 was determined by qPCR and immunoblotting. GAPDH was used as an internal control. d Expression of NKG2D was not found on the surface of tumor cell lines by flow

cytometry with anti-human NKG2D antibody. e NKG2DLs, MICAα1-2, and MICAα1-3 showed no binding with tumor cell lines. f Compared with blank control and isotype control, 2A9-MICA and 2A9 showed similar binding with BCMA+ cell lines RPMI-8226 and NCI-H929, but 2A9-MICAα1-2 had a higher binding rate than that of 2A9-MICA and 2A9. g Affinity of 2A9-MICA and 2A9-MICAα1-2 to NKG2D was analyzed by surface plasmon resonance. NKG2D protein was covalently bonded to the CM5 sensor chip, and the tested concentrations of 2A9-MICA and 2A9-MICAα1-2 were 1000 nM-31.25 nM and 1000 nM-15.625 nM, respectively; the dilution factor was 2. T-test analysis was performed in qPCR, and data were given as the mean with SEM (n=3). *p<0.05, **p<0.01, ***p<0.001, NS means no significance.

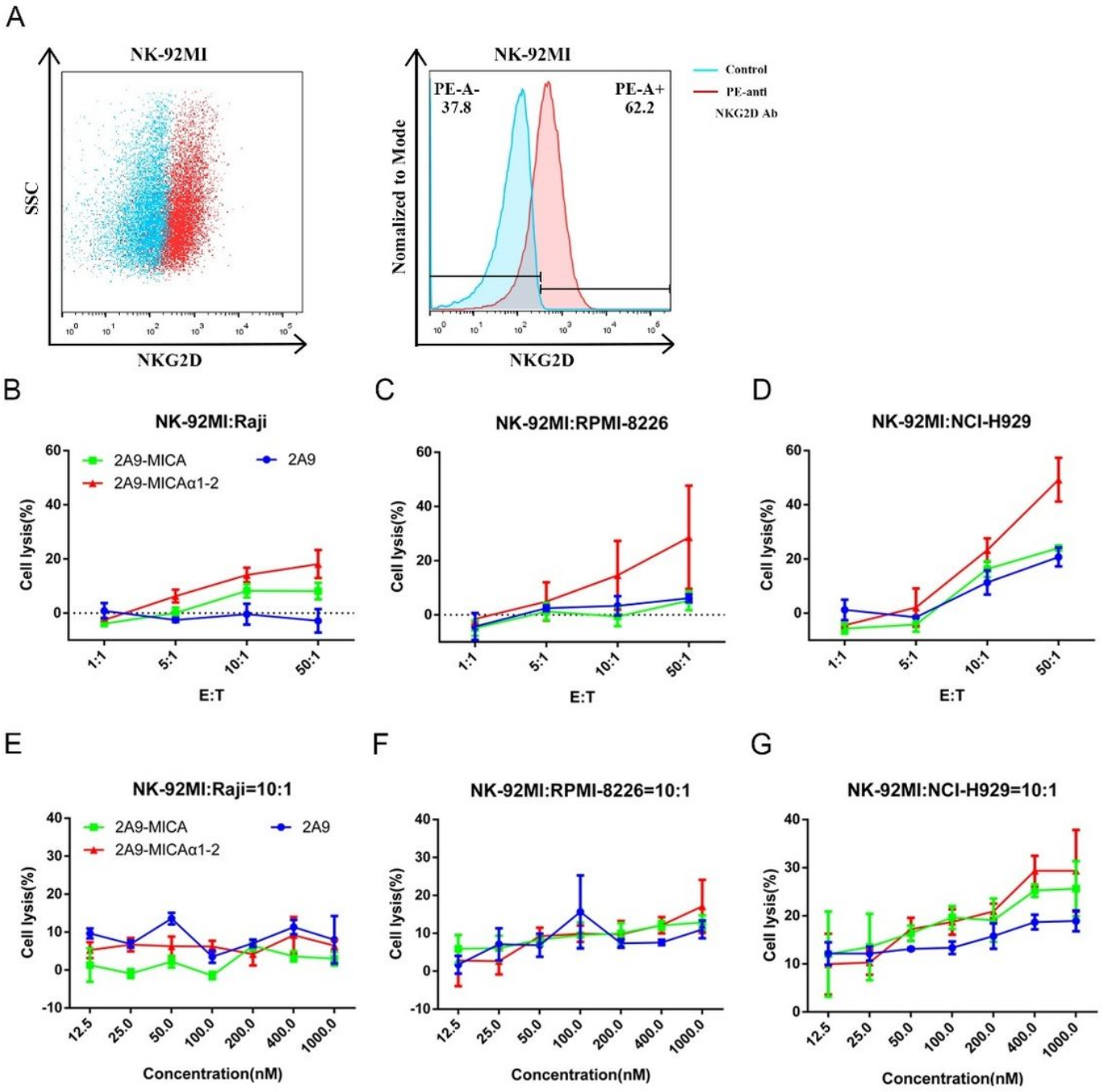

Figure 3

2A9-MICAα1-2 effectively mediated NK-92MI cytotoxicity against BCMA+ MM cells. a The expression abundance of NKG2D in NK-92MI was identified by flow cytometry with PE-anti-human NKG2D antibody. b, c, d NK-92MI cells were co-cultured with tumor cells at E:T ratios of 1:1, 5:1, 10:1, and 100:1 in an optimal concentration of 2A9, 2A9-MICA, and 2A9-MICAα1-2. e, f, g Activated NK-92MI-dependent cytotoxicity was evaluated with a gradient concentration of 2A9, 2A9-MICA, and 2A9-MICAα1-2 at the E:T ratio of 10:1. Data were given as the mean with SEM (n=3). *p<0.05, **p<0.01, ***p<0.001, NS means no significance.

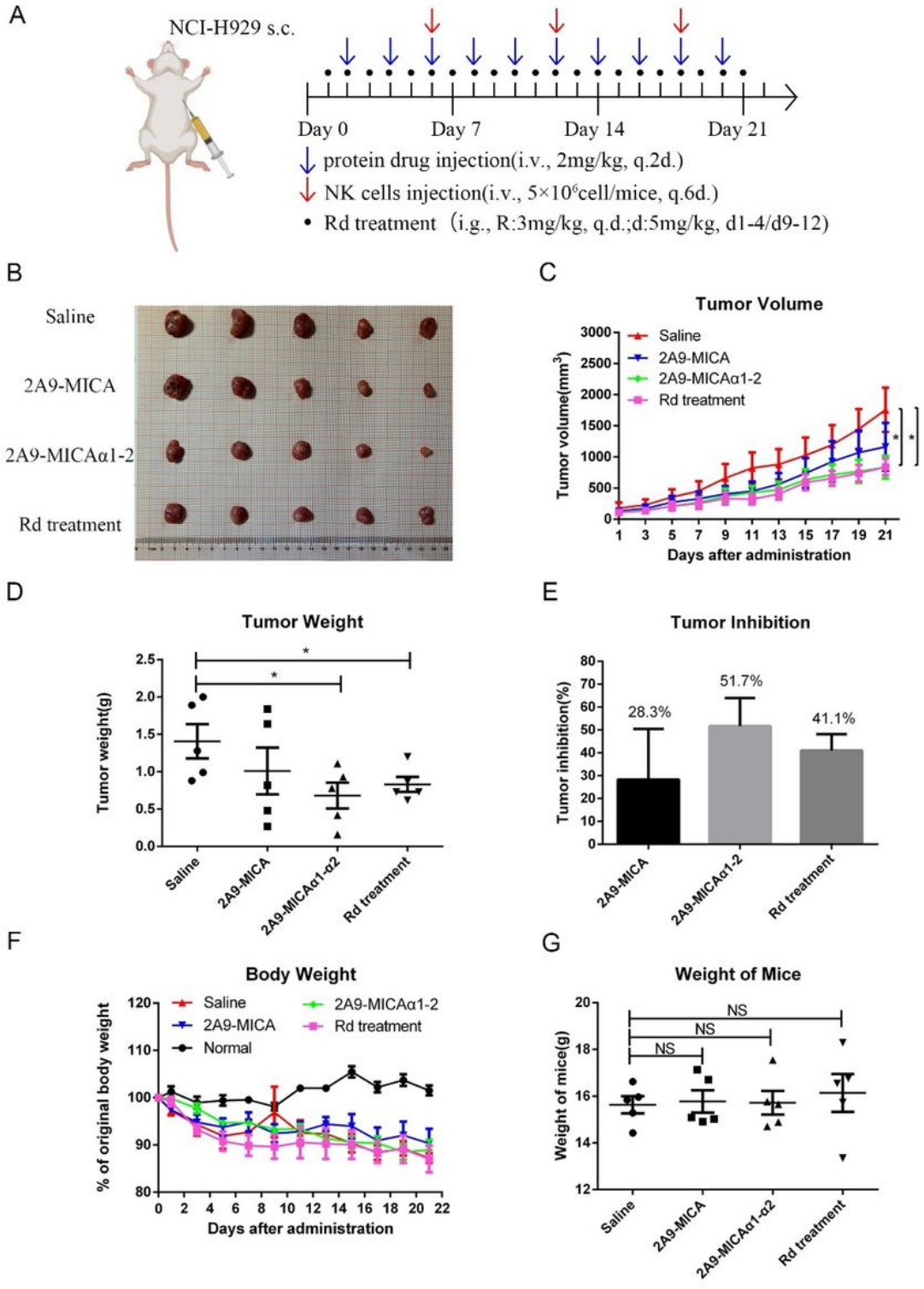

Figure 4

2A9-MICAα1-2 behaved superior anti-myeloma efficacy in NCI-H929-bearing nude mice. a Construction of NCI-H929 subcutaneous xenograft model in nude mice and scheme of administration or injection. b The photograph of tumor tissue showing the results visually. c Tumor growth curve of mice treated with saline, 2A9-MICA, 2A9-MICAα1-2, and Lenalidomide combined with Dexamethasone. d, e Individual tumor weights in each treatment group were measured on day 22, and the corresponding tumor inhibition rates of different drug groups were calculated. f, g The whole body weight of normal and experimental mice was monitored during the administration, and we analyzed the last record of body weight on day 21. There was no difference within experimental groups. T-test analysis was performed, and data were given as the mean with SEM (n=5). *$p<0.05$, **$p<0.01$, ***$p<0.001$, NS means no significance.

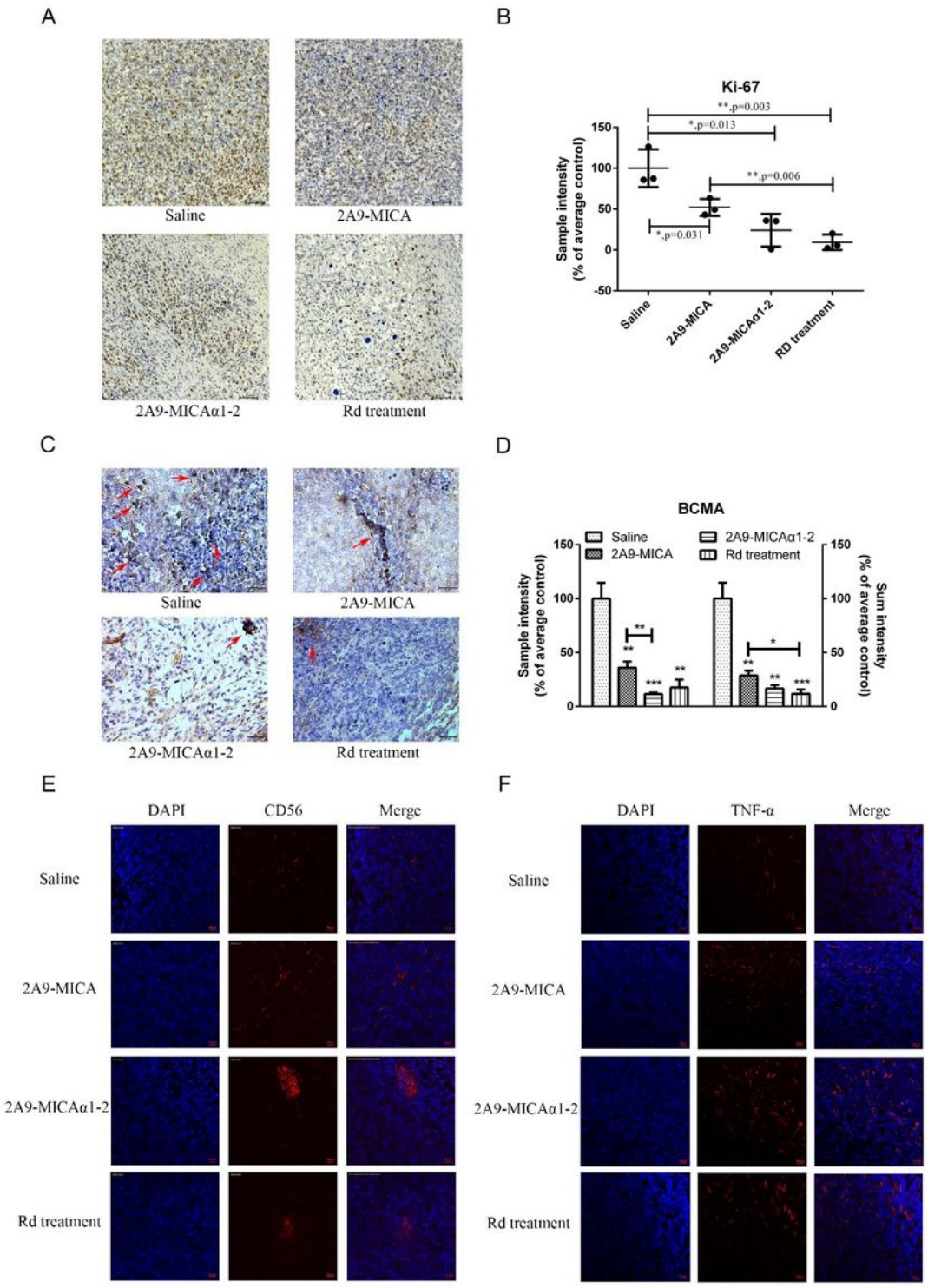

Figure 5

2A9-MICAα1-2 effectively reduced malignancy of MM and fully activated NK cells. a, c Expression of Ki-67 and BCMA in paraffin sections of NCI-H929 xenograft tumor identified with corresponding antibodies (brown staining) by immunohistochemistry (a, 200×, 50 μm; c, 400×, 20 μm). b, d The sample or sum intensity (% of average control) analysis was performed by Image-Pro Plus software. e, f Immunofluorescence staining of the human NK cell biomarker CD56 (e) and the level of cytokine TNF-α

(f) released by CD56+ NK cells within the tumor microenvironment (200×, 20 μm). T-test analysis was performed, and data were given as the mean with SD (n=3). *p<0.05, **p<0.01, ***p<0.001, NS means no significance.

Supplementary Files

This is a list of supplementary files associated with this preprint. Click to download.

- FigS1.jpeg
- FigS2.jpeg
- FigS3.jpeg
- Highlights.jpeg